JOURNAL OF SPACECRAFT AND ROCKETS
Vol. 32, No. 5, September–October 1995

# Fiber Contribution to Modal Damping of Polymer Matrix Composite Panels

S. Yarlagadda* and G. Lesieutre†
*Pennsylvania State University, University Park, Pennsylvania 16802*

**An analytical method to determine the modal frequencies and damping of flexural vibration of continuous fiber-reinforced composite panels has been developed. Fiber damping effects are included in this method. Damped panel vibration modes are found using a higher-order laminate theory and the Rayleigh-Ritz method with complex eigenvalue analysis. Fiber contribution to modal damping was found to be significant in vibration modes involving longitudinal deformation of fibers. For a $[0]_8$ P100/3501-6-square cantilevered laminate, in vacuum and at room temperature (20°C), the predicted first mode damping showed an increase of 77% by including fiber damping. The use of bromine-intercalated P100 fibers resulted in a further predicted increase of 438% in the first mode damping at room temperature. Effects of changes in ply orientation, temperature, and thickness of the laminate on the fiber contribution to damping were examined. Fiber contribution to the damping of an angle-ply laminate can be estimated from the mode shapes and ply orientation of the laminate. Damping of modes exhibiting nearly pure bending or a combination of bending and twisting can be significantly improved by use of treated (intercalated) fibers.**

## Nomenclature

| | |
|---|---|
| $A$ | = area of laminate, m$^2$ |
| $C_{ij}$ | = stiffness coefficients of the $k$th lamina, N/m$^2$ |
| $c$ | = volume fraction |
| $E_L$ | = longitudinal Young's modulus, N/m$^2$ |
| $h$ | = laminate thickness, m |
| $h_k$ | = thickness of the $k$th lamina |
| $K_T$ | = plane strain bulk modulus, N/m$^2$ |
| $M, N$ | = number of modes in the $X$ and $Y$ directions, respectively |
| $n$ | = number of laminae or layers |
| $q$ | = degrees of freedom ($W$, $u$, $v$, and $w$) |
| $T_{mn}$ | = unknown coefficients (amplitudes of assumed mode shapes) |
| $\bar{U}, \bar{V}, \bar{W}$ | = displacements in $x$, $y$, and $z$ directions, respectively |
| $U$ | = strain energy, J |
| $\Delta U$ | = energy dissipated, J |
| $u, v, w$ | = shear deformations in $x$, $y$, and $z$ directions, respectively |
| $X(x), Y(y)$ | = assumed beam mode shapes |
| $\zeta$ | = modal damping ratio |
| $\eta$ | = loss factor |
| $\lambda$ | = complex frequency, Hz |
| $\mu_{LT}$ | = longitudinal shear modulus, N/m$^2$ |
| $\mu_{TT}$ | = transverse shear modulus, N/m$^2$ |
| $\nu_{LT}$ | = longitudinal Poisson's ratio |
| $\xi$ | = $z/h$ |
| $\psi$ | = specific damping capacity |

*Subscripts*

| | |
|---|---|
| $f$ | = fiber |
| $m$ | = matrix |

## I. Introduction

VIBRATION damping is an important design requirement in many new applications of composite materials. Research on analytical and experimental characterization of damping in composites has been driven by several potential applications. For example, the three key material property requirements for large precision space structures are high stiffness-to-weight ratio, a low thermal expansion coefficient, and high damping. Design optimization for such parameters is feasible only with composites.

The dynamic mechanical behavior of fiber-reinforced composite structural materials is governed primarily by their stiffness and damping properties. One of the goals of composite micromechanics has been to predict the stiffness and damping properties from constituent material properties and the interaction between the constituent materials.[1–3] Several review articles on the stiffness and damping properties of polymer matrix composites are available in the literature.[4–6] In general, a two-part approach has been followed in analytical modeling. The first part involves micromechanical modeling to predict the stiffness and damping properties of the composite (lamina) from the fiber and matrix properties. The second part involves predicting the dynamics of the laminate based on the geometry, orientation of piles, and lamina stiffness and damping properties. This general approach is also followed herein.

Several micromechanical models predicting lamina stiffness properties from the fiber and matrix properties are available in the literature.[1,2,7–9] However, prediction of lamina damping properties from the fiber and matrix damping properties has not received similar attention, mainly because of the difficulty in experimentally measuring the damping properties of the fibers. Also, matrix damping is generally higher than fiber damping. For these reasons, the fiber damping contribution to the overall damping of composites is usually neglected. Micromechanical models incorporating fiber damping have been developed for discontinuous fiber composites, with the continuous fibers being a limiting case.[10–12]

In many composites, most of the strain energy is stored in the fibers, so that improvements in fiber damping could translate into significant increases in composite damping. It is important to examine the contribution of fiber to composite damping, especially in modes involving significant fiber strain energy. In recent years, damping of graphite fibers intercalated with bromine has been experimentally measured[13,14] and shown to be at least an order of magnitude greater than damping in untreated graphite fibers.[15] The effect of using treated fibers on the overall composite damping needs to be examined.

The objective of this work was to understand the fiber contribution to damping of polymer-matrix composites. Fiber damping was characterized by an experimentally measured[13–15] loss factor. Effects of ply orientation, temperature, and thickness were also examined.

Received Oct. 22, 1992; revision received Sept. 1, 1993; accepted for publication Sept. 3, 1993. 

*Graduate Student, Department of Aerospace Engineering. Member AIAA.

†Assistant Professor, Department of Aerospace Engineering. Senior Member AIAA.

## II. Theory

Consider a midplane symmetric anisotropic laminate (panel) of thickness $h$, referred to an $x$, $y$, $z$ system of Cartesian coordinates, so that $z = 0$ at the midplane of the laminate. Midplane symmetric laminates are considered in order to eliminate bending–stretching coupling. Transverse shear strains on the top and bottom surfaces of the laminate are assumed to be zero, however, inplane shear strains are not necessarily zero.

The modal specific damping capacity (SDC) $\psi$ is defined as

$$\psi = \frac{\Delta U}{U} = \frac{\text{Energy dissipated in a cycle of steady vibration at a modal frequency}}{\text{Maximum strain energy}} \tag{1}$$

### A. Prediction of Lamina Elastic Properties

Several models are available for the calculation of lamina elastic properties from the constituent fiber and matrix properties. They can be classified broadly under two basic approaches: 1) mechanics of materials[1,7] and 2) elasticity.[2,7]

Most models assume the fibers to be isotropic, which is inappropriate in the case of anisotropic fibers like graphite, boron, etc. This assumption, however, simplifies the problem considerably and provides reasonable estimates for the longitudinal properties of the lamina, but poor estimates of the transverse properties. In recent years, several theories have been developed based on fibers that are transversely isotropic or anisotropic.[7–9]

Hashin[8] developed a transversely isotropic analogue to the composite cylinder assemblage (CCA) model. A simple scheme to transform results and analysis procedures for isotropic fibers and matrix into corresponding results and procedures for transversely isotropic fibers and matrix is outlined.

Using a wave-scattering method, Datta et al.[9] derived dispersion relationships for waves propagating perpendicular to continuous fibers, oriented unidirectionally. The fibers were assumed to be transversely isotropic. Relationships predicting the effective composite elastic constants are obtained as shown here:

$$\mu_{LT}/\mu_m = \frac{1 + c_f[(m-1)/(m+1)]}{1 - c_f[(m-1)/(m+1)]}; \qquad m = \mu_{f_{LT}}/\mu_m \tag{2a}$$

$$\mu_{TT}/\mu_m = 1 + \frac{2c_f(\mu_{f_{TT}} - \mu_m)(\lambda_m + 2\mu_m)}{2\mu_m(\lambda_m + 2\mu_m) + (1 - c_f)(\mu_{f_{TT}} - \mu_m)(\lambda_m + 3\mu_m)} \tag{2b}$$

$$\nu_{LT} = \nu_m(1 - c_f) + \nu_{LT_f}c_f + \frac{c_f(1 - c_f)(\nu_{LT_f} - \nu_m)(1/k_m - 1/k_{T_f})}{(1 - c_f)/k_{T_f} + c_f/k_m + 1/\mu_m} \tag{2c}$$

$$\nu_{TL} = \nu_{LT}E_T/E_L \tag{2d}$$

$$K_T = \lambda_m + \mu_m + (\lambda_m + 2\mu_m)\frac{c_f(k_{T_f} - \lambda_m - \mu_m)}{(1 - c_f)k_{T_f} + c_f\lambda_m + (1 + c_f)\mu_m} \tag{2e}$$

$$E_L = E_m(1 - c_f) + E_{L_f}c_f + \frac{4c(1 - c_f)(\nu_{LT_f} - \nu_m)^2}{(1 - c_f)/k_{T_f} + c_f/k_m + 1/\mu_m} \tag{2f}$$

### B. Prediction of Lamina Dynamic Properties

Hashin developed a correspondence principle[16] to extend elastic models to predict the dynamic response of composites. According to this principle, effective dynamic moduli of linear viscoelastic composites can be determined on the basis of analytical expressions for the effective elastic moduli of composites. The dynamic modulus is a complex quantity, and the complex part is a measure of damping. In general

$$P = P'(1 + i\eta) = P' + iP''; \qquad \eta = \psi/2\pi = P''/P' = 2\zeta \tag{3}$$

where $P$ is a dynamic modulus, $P'$ a storage modulus, and $P''$ a loss modulus.

To calculate the lamina complex moduli, the fiber and matrix complex moduli are determined from the measured elastic moduli and loss factors. The fiber and matrix elastic moduli in the lamina elastic property prediction model (Eqs. 2a–2f) are replaced by the corresponding complex moduli.

It should be emphasized that the correspondence principle is valid only for steady-state, time harmonic, forced vibrations of a linear viscoelastic material. Therefore, the application of this principle to the free damped vibration of laminates is approximate, and the error involved depends on the magnitude of damping. Struik[17] showed that the error becomes significant only when $\psi$ is of the order of 0.5. For most materials, including composites, $\psi$ is much smaller (typically of the order of $10^{-2}$), and the approximation error is negligible.

### C. Dynamic Model of Laminated Plates

To model the dynamic behavior of laminated composite plates subject to various boundary conditions, the Rayleigh–Ritz method was used. Shear deformation and rotary inertia effects were accounted for using a higher-order plate theory.

#### 1. *Higher-Order Plate Theory*

The higher-order shear deformation theory used in this investigation is a four-degree-of-freedom theory, based on cubic inplane displacements and parabolic normal displacements.[18]

The displacements are of the form

$$\begin{aligned} \bar{U} &= -zW_{,x} - \xi(1 - \xi^2/3)u \\ \bar{V} &= -zW_{,y} - \xi(1 - \xi^2/3)v \\ \bar{W} &= W + (1 - \xi^2)w \end{aligned} \tag{4}$$

where $W$, $u$, $v$, and $w$ are functions of $x$, $y$, and $t$. The form in Eq. (4) assumes there are no initial inplane displacements in the laminate. These displacements could be included to make the model more complete, but this would increase the number of degrees of freedom to six, unnecessarily increasing the size of the problem.

The constitutive law for the $k$th lamina can be written as

$$\begin{bmatrix} \sigma_x \\ \sigma_y \\ \sigma_z \\ \tau_{xy} \end{bmatrix} = \begin{bmatrix} C_{11} & C_{12} & C_{13} & C_{16} \\ C_{12} & C_{22} & C_{23} & C_{26} \\ C_{13} & C_{23} & C_{33} & C_{36} \\ C_{16} & C_{26} & C_{36} & C_{66} \end{bmatrix}^k \begin{bmatrix} \varepsilon_x \\ \varepsilon_y \\ \varepsilon_z \\ \gamma_{xy} \end{bmatrix}^k$$

$$\begin{bmatrix} \tau_{yz} \\ \tau_{xz} \end{bmatrix}^k = \begin{bmatrix} C_{44} & C_{45} \\ C_{45} & C_{55} \end{bmatrix}^k \begin{bmatrix} \gamma_{yz} \\ \gamma_{xz} \end{bmatrix}^k \tag{5}$$

Defining

$$\begin{aligned} F_{ij} &= -\sum_{k=1}^{n} C_{ij}^k \int_{h_{k-1}}^{h_k} pz\,dz & \begin{pmatrix} i = 1,2,3,6 \\ j = 1,2,6 \end{pmatrix} \\ F_{i3} &= \sum_{k=1}^{n} C_{i3}^k \int_{h_{k-1}}^{h_k} q'z\,dz & (i = 1,2,3,6) \\ G_{ij} &= -\sum_{k=1}^{n} C_{ij}^k \int_{h_{k-1}}^{h_k} p^2\,dz & \begin{pmatrix} i = 1,2,6 \\ j = 1,2,6 \end{pmatrix} \\ G_{i3} &= \sum_{k=1}^{n} C_{i3}^k \int_{h_{k-1}}^{h_k} pq'\,dz & (i = 1,2,6) \\ D_{ij} &= \sum_{k=1}^{n} C_{ij}^k \int_{h_{k-1}}^{h_k} z^2\,dz & \begin{pmatrix} i = 1,2,3,6 \\ j = 1,2,3,6 \end{pmatrix} \\ E_{ij} &= \sum_{k=1}^{n} C_{ij}^k \int_{h_{k-1}}^{h_k} q^2\,dz & \begin{pmatrix} i = 4,5 \\ j = 4,5 \end{pmatrix} \end{aligned} \tag{6}$$

The strain energy of the laminate is given by

$$U = \frac{1}{2}\int_A \{D_{11}(W_{,xx})^2 + 2D_{12}W_{,xx}W_{,yy} + D_{22}(W_{,yy})^2 + 4D_{16}W_{,xx}W_{,xy} + 4D_{26}W_{,yy}W_{,xy} + 4D_{66}(W_{,xy})^2 + (2/h^2)(D_{13}wW_{,xx} + D_{23}wW_{,yy} + 2D_{63}wW_{,xy}) - G_{11}(u_{,x})^2 - 2G_{12}u_{,x}v_{,y} - G_{22}(v_{,y})^2 - G_{13}(w/h)u_{,x} - G_{23}(w/h)v_{,y} - G_{63}(w/h)(u_{,y} + v_{,x}) - 2G_{16}u_{,x}(u_{,y} + v_{,x}) - 2F_{33}(w^2/h^2) - 2G_{26}v_{,y}(u_{,y} + v_{,x}) - G_{66}(u_{,y} + v_{,x})^2 - 2F_{11}u_{,x}W_{,xx} - 2F_{22}v_{,y}W_{,yy} - 2F_{12}(u_{,x}W_{,xx} + v_{,y}W_{,yy}) - F_{13}(w/h)W_{,xx} - F_{23}(w/h)W_{,yy} - 2F_{31}(w/h^2)u_{,x} - 2F_{32}(w/h^2)v_{,y} - 2F_{63}(w/h)W_{,xy} - 2F_{16}[(u_{,y} + v_{,x})W_{,xx} + 2u_{,x}W_{,xy}] - 2F_{26}[(u_{,y} + v_{,x})W_{,yy} + 2u_{,y}W_{,xy}] - 4F_{66}(u_{,y} + v_{,x})W_{,xy} - 2F_{36}(w/h^2)(u_{,y} + v_{,x}) + E_{44}[-(v/h) + w_{,y}]^2 + E_{55}[-(u/h) + w_{,x}]^2 + 2E_{45}[-(v/h) + w_{,y}][-(u/h) + w_{,x}]\}\,dA \quad (7)$$

The kinetic energy is obtained as

$$\mathrm{KE} = \frac{1}{2}\omega^2\int_A [\rho_A(W_{,x})^2 + \rho_F(u)^2 + 2\rho_B(uW_{,x}) + \rho_A(W_{,y})^2 + \rho_F(v)^2 + 2\rho_B(uW_{,x}) + \rho_C(W)^2 + \rho_E(w)^2 + 2\rho_D(wW)]\,dA \quad (8)$$

where

$$(\rho_A, \rho_B, \rho_C, \rho_D, \rho_E, \rho_F) = \int_{-h/2}^{+h/2} \rho_o(z^2, pz, 1, q, q^2, p^2)\,dz$$

and

$$p = \xi(1 - \xi^2/3); \qquad q = (1 - \xi^2); \qquad q' = dq/d\xi$$

*2. Solution Procedure*

Mode shapes were assumed and substituted directly in Eqs. (7) and (8). Evaluating the integrals and minimizing using Hamilton's principle[19] yielded an eigenvalue problem in the unknown coefficients. The assumed shapes used were beam mode shape combinations[20] appropriate to the boundary conditions of the laminate being modeled. The mode shapes were of the general form

$$q = \sum_{m=1}^{M}\sum_{n=1}^{N} T_{mn}X_m(x)Y_n(y) \qquad (q = W, u, v, w) \quad (9)$$

where $T_{mn}$ are the unknown coefficients.

Substitution of these modes in the strain and kinetic energy equation and subsequent minimization, after application of the correspondence principle, leads to a complex eigenvalue problem in $4 \times M \times N$ linear equations in the unknown coefficients $T_{mn}$. The eigenvalues and eigenvectors were calculated using a standard complex eigenvalue extraction routine.

### D. Prediction of Modal Damping

The specific damping capacity (SDC) is defined as the ratio of the strain energy dissipated during a cycle to the maximum strain energy (Eq. (1)). In the complex modulus approach, the loss factor is the ratio of the imaginary part of the modulus to the real part.

The most common approach to calculate the overall specific damping capacity, the modal strain energy method (MSE), involves determining the energy dissipated in the laminate during a cycle by summing the components of energy dissipated caused by each material in each stress component.[21] The energy dissipated is calculated from

$$\Delta U = \Delta U_x + \Delta U_y + \Delta U_{yz} + \Delta U_{xz} + \Delta U_{xy} \quad (10)$$

A slightly modified approach is more accurate. Instead of separately calculating the components of energy dissipated, the complex moduli are used to construct a complex stiffness matrix and the corresponding complex eigenvalues; i.e., formulate a complex eigenvalue problem—the complex frequency method (CFM). The complex eigenvalue would be of the form

$$\lambda = -\zeta\omega \pm i\omega\sqrt{1 - \zeta^2} \quad (11)$$

from which the damped frequency and damping ratio $\zeta$ can be calculated.

The preceding approach was used because it has the following advantages: 1) the damped frequencies are directly calculated, and 2) it is computationally simpler, because only the complex eigenvalues have to be calculated, and not the energy dissipated.

## III. Results and Discussion

### A. Flexural Vibration Frequencies and Damping

Lin et al.[21] used a damped finite element model in conjunction with the MSE to predict vibration and damping parameters of free–free laminates. However, their results were not based on fiber and matrix dynamic properties, but those of the composite. The results obtained from the present Rayleigh–Ritz method are compared with their predictions. The laminate data are listed in Tables 1 and 2.

For the two laminates considered, Tables 3 and 4 list the predicted flexural vibration and damping results. Because the laminates are free–free, the first three modes are rigid body modes and have zero frequencies. Table 3 also lists natural frequencies as predicted by ANSYS, using a composite element, STIF46. The agreement between the frequencies predicted by the present model, ANSYS, and by Lin et al.[21] is quite good. Note that results from both ANSYS and the present model are for a fiber volume fraction of 0.5.

Damping capacities predicted for the aforementioned laminates have been presented in Table 4. Damping predictions of the present model compare well with results from Lin et al.[21] It should be noted that in almost all cases, the damping predictions of the present model are slightly higher than predictions by Lin et al.[21] This may be attributed to the use of CFM, which, unlike the MSE used by Lin et al.,[21] takes into account all possible modes of energy dissipation (including transverse shear and through-the-thickness deformation), and hence will predict higher values of damping than the MSE.

### B. Fiber Contribution to Damping

To investigate the fiber contribution to laminate damping, the relative effects of treated (intercalated) and untreated fibers on the modal damping capacities of a square cantilevered $[0]_8$ P100/3501-6

**Table 1 HMS/DX210 elastic and dynamic properties[21] for fiber volume fraction, 0.5**

| | Material | | | | | | |
|---|---|---|---|---|---|---|---|
| | $E_L$, GPa | $E_T$, GPa | $G_{LT}$, GPa | $\psi_L$, % | $\psi_T$, % | $\psi_{LT}$, % | $\nu_{LT}$ |
| HMS/DX210 | 172.7 | 7.20 | 3.76 | 0.45 | 4.22 | 7.05 | 0.3 |

**Table 2 Laminate geometries and layups used to compare present model predictions[a] with those of Lin et al.[21]**

1) All 0-ply
8 layers, 178-mm-square; thickness, 1.58 mm
Density, 1566 kg/m$^3$; fiber volume fraction, 0.516
2) $[0, 90, \pm 45]_s$
215-mm-square; thickness, 1.62 mm
Density, 1551.4 kg/m$^3$; fiber volume fraction, 0.494

[a]Boundary conditions: All four sides free.

**Table 3 Comparison of predicted flexural vibration frequencies with those of ANSYS and lin et al.[21]**

| Laminate | Mode number | Frequency, Hz | | | |
|---|---|---|---|---|---|
| | | Experiment[21] | Lin et al.[21] | Present model | ANSYS |
| All 0-ply 8 layers (0.516)[a] | 4 | 81.50 | 83.57 | 81.56 | 80.01 |
| | 5 | 107.4 | 118.42 | 110.53 | 106.66 |
| | 6 | 196.6 | 207.79 | 202.08 | 192.49 |
| | 7 | 295.5 | 329.41 | 306.19 | 288.53 |
| | 8 | 382.5 | 419.83 | 400.72 | 371.56 |
| | 9 | 531.0 | 546.93 | 540.57 | 518.32 |
| $[0, 90, \pm 45]_s$ (0.494)[a] | 4 | 77.80 | 86.33 | 87.77 | 85.411 |
| | 5 | 202.7 | 224.49 | 227.76 | 219.69 |
| | 6 | 258.0 | 280.42 | 285.47 | 272.18 |
| | 7 | 298.7 | 298.81 | 303.44 | 292.38 |
| | 8 | 322.0 | 348.36 | 355.50 | 338.63 |
| | 9 | 496.7 | 512.24 | 525.10 | 487.64 |

[a]Actual fiber volume fraction. Volume fraction considered in present method is 0.5.

**Table 4 Comparison of predicted modal damping capacities with those of Lin et al.[21]**

| Laminate | Mode number | Specific damping capacity, $\psi$, % | | |
|---|---|---|---|---|
| | | Experiment[21] | Lin et al.[21] | Present model |
| All 0-ply 8 layers (0.516)[a] | 4 | 7.0 | 6.76 | 6.88 |
| | 5 | 4.9 | 4.28 | 4.22 |
| | 6 | 5.4 | 5.89 | 6.07 |
| | 7 | 4.7 | 4.13 | 4.23 |
| | 8 | 4.8 | 5.11 | 5.33 |
| | 9 | —— | 0.47 | 0.52 |
| $[0, 90, \pm 45]_s$ (0.494)[a] | 4 | 1.40 | 1.44 | 1.47 |
| | 5 | 0.88 | 0.93 | 0.95 |
| | 6 | 0.65 | 0.63 | 0.67 |
| | 7 | 1.26 | 1.23 | 1.27 |
| | 8 | 0.99 | 0.98 | 0.99 |
| | 9 | —— | 0.92 | 0.98 |

[a]Actual fiber volume fraction. Volume fraction considered present method is 0.5.

**Table 5 Dynamic properties of the fiber and matrix[13–15]**

| Material | $\psi_L$, % | $\psi_T$, % | $\psi_{LT}$, % |
|---|---|---|---|
| Temperature, −50°C (corresponds to peak fiber damping) | | | |
| Fiber: P100 treated graphite | 2.89 | —— | —— |
| Fiber: P100 untreated graphite | 0.18 | —— | —— |
| Matrix: Hercules 3501-6 | 25.76 | 25.76 | 28.27 |
| Temperature, 20°C | | | |
| Fiber: P100 treated graphite | 1.00 | —— | —— |
| Fiber: P100 untreated graphite | 0.15 | —— | —— |
| Matrix: Hercules 3501-6 | 18.96 | 18.96 | 20.74 |

laminate are examined. Dynamic properties of fiber and matrix are listed in Table 5 (Refs. 13–15). Fiber and matrix damping capacities in the $LZ$ and $TZ$ directions were unavailable. Table 6 lists the predicted flexural vibration frequencies and damping capacities for the first five modes.

Despite the large difference in fiber and matrix damping, neglecting treated fiber damping causes a 44% underprediction in the damping capacity of the first mode. For the other modes, the errors are much smaller, because modes two, three, four, and five are twisting modes, and consequently they are dominated by matrix shear damping. Mode 6 shows a 25% error, because it is a bending mode. The assumption of zero fiber damping seems to be valid for twisting modes of vibration, which are dominated by matrix shear, but invalid for longitudinal bending modes.

The use of treated fiber produces significant increases in the overall damping capacities of the laminate. Percentage increases range

**Table 6 Predicted flexural vibration frequencies and damping capacities for a $[0]_8$ square cantilever laminate; temperature, 20°C**

| Mode number | Frequency, Hz | Modal damping capacity, $\psi$, % | | |
|---|---|---|---|---|
| | | Matrix damping only | Untreated fiber + matrix | Treated fiber + matrix |
| 1 | 121.46 | 0.192 | 0.339 | 1.18 |
| 2 | 130.86 | 2.59 | 2.72 | 3.44 |
| 3 | 182.85 | 8.15 | 8.23 | 8.59 |
| 4 | 326.35 | 10.89 | 10.91 | 11.03 |
| 5 | 556.08 | 11.39 | 11.39 | 11.43 |
| 6 | 752.57 | 0.428 | 0.573 | 1.39 |

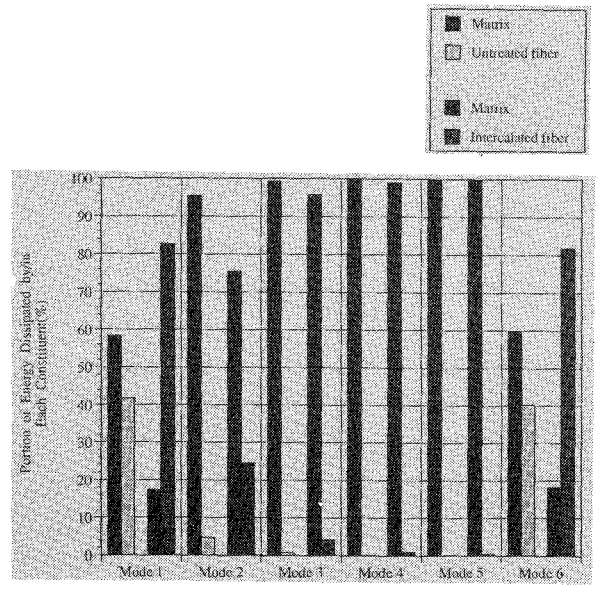


**Fig. 1 Comparison of fiber and matrix contributions to damping of $[0]_8$ square cantilever laminate at temperature 20°C.**

from 250% for mode 1 to 1.1% for mode 4. Figure 1 shows fractions of the energy dissipated in each constituent, for modes 1–6. As expected, the twisting modes show negligible to small increases, and in the bending modes, mode 1 (250%) and 6 (140%) show the maximum increases. These increases occur although the matrix damping is much higher than that of the treated fiber. This result highlights the error involved in the assumption of negligible fiber damping.

The significant fiber contribution to the bending modes and smaller contribution to the twisting modes suggests that the laminate mode shape can serve as a good indicator of the contribution of the fiber to the overall modal damping. This hypothesis was tested further by examining the dynamic characteristics of laminates for different ply orientations.

**Table 7 Predicted flexural vibration frequencies and damping capacities for a $[(0, 90)_2]_s$ square cantilever laminate; temperature, 20°C**

| Mode number | Frequency, Hz | Modal damping capacity, $\psi$, % | | |
|---|---|---|---|---|
| | | Matrix damping only | Untreated fiber + matrix | Treated fiber + matrix |
| 1 | 101.11 | 0.289 | 0.436 | 1.27 |
| 2 | 112.77 | 3.68 | 3.80 | 4.47 |
| 3 | 462.88 | 1.30 | 1.43 | 2.21 |
| 4 | 626.65 | 0.575 | 0.718 | 1.53 |
| 5 | 640.16 | 1.30 | 1.44 | 2.22 |
| 6 | 812.57 | 2.49 | 2.62 | 3.34 |

**Table 8 Predicted flexural vibration frequencies and damping capacities for a $[45, -45)_2]_s$ square cantilever laminate; temperature, 20°C**

| Mode number | Frequency, Hz | Modal damping capacity, $\psi$, % | | |
|---|---|---|---|---|
| | | Matrix damping only | Untreated fiber + matrix | Treated fiber + matrix |
| 1 | 57.284 | 1.81 | 1.94 | 2.69 |
| 2 | 211.52 | 0.724 | 0.866 | 1.67 |
| 3 | 329.19 | 2.39 | 2.52 | 3.24 |
| 4 | 546.22 | 1.11 | 1.25 | 2.03 |
| 5 | 688.99 | 1.26 | 1.40 | 2.18 |
| 6 | 1053.2 | 1.66 | 1.79 | 2.55 |

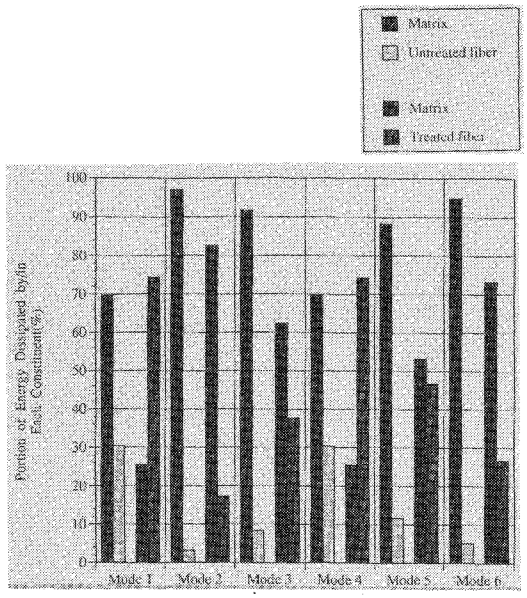


**Fig. 2 Comparison of fiber and matrix contributions to damping of $[(0, 90)_2]_s$ square cantilever laminate at temperature 20°C.**

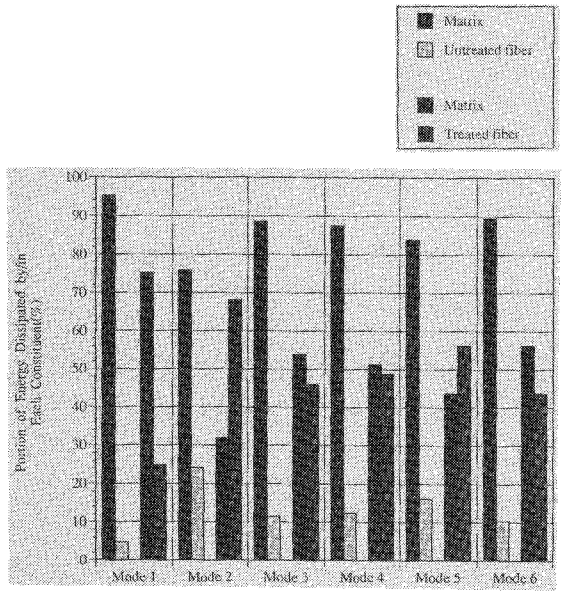


**Fig. 3 Comparison of fiber and matrix contributions to damping of $[(\pm 45)_2]_s$ square laminate at temperature 20°C.**

### C. Effect of Ply Orientation on Fiber Contribution

The results of the previous section indicate that fiber damping effects should not be neglected in bending modes of vibration of the $[0]_8$-ply laminate. It follows that fiber damping effects, in general, should not be neglected for modes causing longitudinal fiber deformation, regardless of the laminate ply orientation. To verify this conclusion, frequency and damping predictions were made for a $[(0, 90)_2]_s$ and a $[(45, -45)_2]_s$ laminate, with the same material properties, geometry, and boundary conditions as the unidirectional ply. Dissipated energy fractions for the fiber and matrix were also calculated.

Table 7 shows the room-temperature modal damping predictions for the $[(0, 90)_2]_s$ laminate. Neglecting the fiber contribution gives lower damping values, with the difference ranging from a high of 34% for mode one to a low of 3% for mode two. Using the treated fiber improves damping significantly for all six modes, ranging from a low of 18% for mode 2 to a high of 91% for mode 1. Figure 2 shows dissipated energy components for the six modes.

Fiber damping effects are most noticeable in modes 1 (30% untreated, 75% treated), 4 (30%, 75%), and 5 (12%, 26%). Modes 1 and 4 are longitudinal bending modes, whereas 5 is a combination of torsion and longitudinal bending, which accounts for the lower fiber contribution. Mode 2 is a twisting mode, 3 is a transverse mode, and 6 is a combination of longitudinal and transverse bending. Hence, modes 2, 3, and 6 can be expected to have matrix dominated damping, which is confirmed in Fig. 2.

Table 8 and Fig. 3 show the predicted modal damping and dissipated energy components for an angle-ply $[(45, -45)_2]_s$ laminate. Using treated fiber improves damping for all the six modes, ranging from a low of 29% for mode 3 to a high of 93% for mode 2. Similar to the $[(0, 90)_2]_s$ case, the mode shape is again found to be a good indicator of the relative contributions of the fiber and matrix to the overall damping. Mode 1 is a longitudinal bending mode, but because the fibers are at 45 deg to the axis, it is actually causing shear deformation, and hence, it is dominated by matrix damping. Mode 2 illustrates the reverse case, where the mode appears to be a torsional mode but actually involves fiber longitudinal deformation. Hence, fiber orientation is of equal importance with the mode shape when estimating damping contributions of the fiber and matrix. Modes 3–6 are all combinations of bending and twisting, and, in all these modes, the untreated fiber contributes approximately 10–15% (between 30% of mode 1 and 2% of mode 2) of the overall damping.

Comparing the damping predictions of each mode for different ply orientations further reinforces this insight. Figures 4 and 5 show comparisons of fiber and matrix contributions to the overall damping, for the different ply orientations, for the first two modes. For both these modes, the different ply orientations have the same mode shapes. In mode 1, changes in ply orientation cause matrix damping effects to increase, which can be inferred from the change of fiber longitudinal deformation in the $[0]_8$-ply case to shear deformation in the $[(45, -45)_2]_s$ case. In mode 2, while the $[0]_8$ and the $[(0, 90)_2]_s$ cases show little contribution from the fiber, the $[(45, -45)_2]_s$ case shows greater fiber damping effect because the orientation of the fiber causes longitudinal deformation. In both modes, use of treated fibers amplifies the fiber damping effects considerably.

Therefore, in vibration modes involving significant longitudinal deformation of the fiber, effects of fiber damping should be included. Fiber contribution to the damping of an angle-ply laminate can be estimated from the mode shapes and ply orientation of the laminate. Damping of modes exhibiting pure bending or a combination of bending and twisting can be significantly improved by use of treated (intercalated) fibers.

### D. Effect of Temperature on Modal Damping

Table 5 (Refs. 13–15) lists the fiber and matrix dynamic properties for two different temperatures and, while the fiber (treated) damping

**Table 9 Predicted flexural vibration frequencies and damping capacities for the $[0]_8$ square cantilever laminate; temperature, −50°C**

| Mode number | Frequency, Hz | Modal damping capacity, $\psi$, % | | |
|---|---|---|---|---|
| | | Matrix damping only | Untreated fiber and matrix | Treated fiber and matrix |
| 1 | 121.46 | 0.26 | 0.44 | 3.11 |
| 2 | 130.86 | 3.53 | 3.69 | 5.99 |
| 3 | 182.86 | 11.11 | 11.19 | 12.40 |
| 4 | 326.41 | 14.85 | 14.87 | 15.28 |
| 5 | 556.18 | 15.52 | 15.53 | 15.69 |
| 6 | 752.57 | 0.58 | 0.76 | 3.37 |

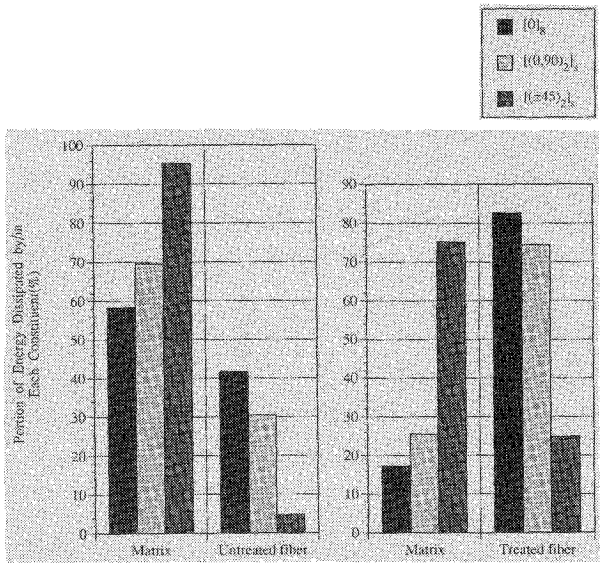


**Fig. 4 Comparison of fiber and matrix contributions to mode 1 of square cantilever laminate with different ply orientations.**

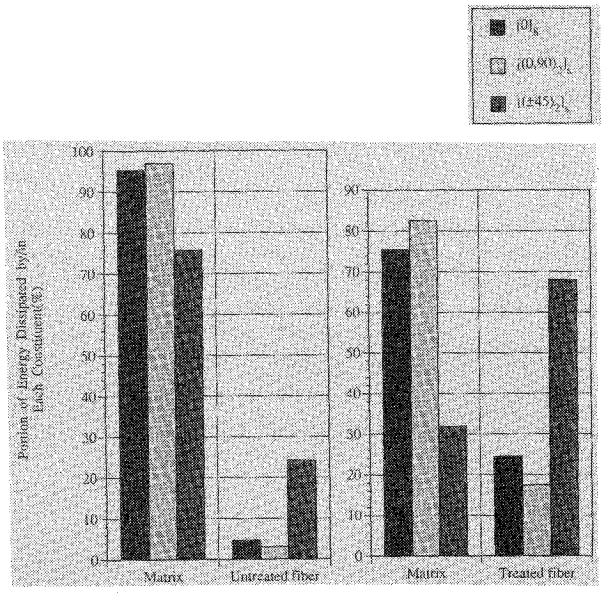


**Fig. 5 Comparison of fiber and matrix contributions to mode 2 of square cantilever laminate with different ply orientations.**

increases three times at the peak (−50°C) compared to room temperature (20°C), the matrix peak value shows a much smaller increase. Hence, it is to be expected that treated fiber damping effects will be more pronounced at temperatures in the vicinity of −50°C than at room temperature.

Table 9 summarizes the results for the square cantilevered $[0]_8$-plylaminate considered in Sec. III.A, but at −50°C. Mode shapes for modes 1–6 are the same as those in Table 6. Comparing modal damping predictions with Table 6 (room temperature = 20°C), similar but more pronounced trends are observed. The overall damping

**Table 10 Predicted flexural vibration frequencies and damping capacities for the thick unidirectional square cantilever laminate at temperature, 20°C**

| Mode number | Frequency, Hz | Modal damping capacity, $\psi$, % | | |
|---|---|---|---|---|
| | | Matrix damping only | Untreated fiber and matrix | Treated fiber and matrix |
| 1 | 1027.8 | 3.18 | 3.28 | 3.89 |
| 2 | 1090.9 | 5.28 | 5.36 | 5.87 |
| 3 | 1540.1 | 9.89 | 9.93 | 10.14 |
| 4 | 2767.8 | 11.94 | 11.95 | 12.0 |
| 5 | 4306.2 | 6.51 | 6.57 | 6.92 |
| 6 | 4376.9 | 7.03 | 7.08 | 7.41 |

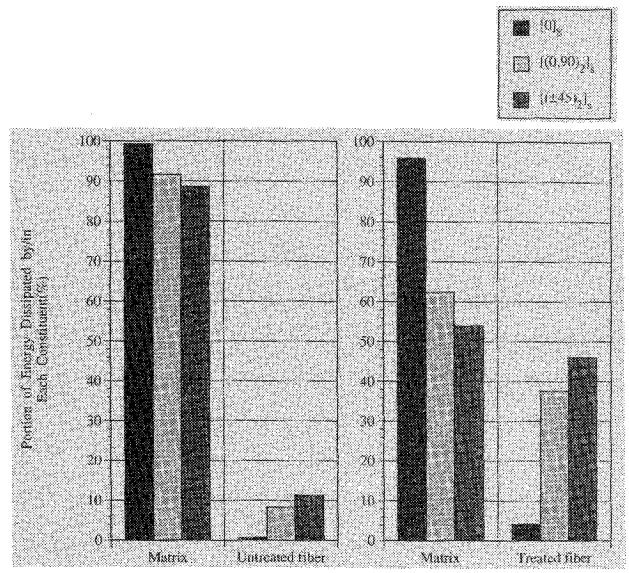


**Fig. 6 Comparison of fiber and matrix contributions to mode 3 of square cantilever laminate with different ply orientations.**

shows large increases (mode 1: 607%; mode 2: 62%; mode 6: 343%) for the bending vibration modes and small increases for the twisting modes (mode 3:11%; mode 4:3%; mode 5:1%), reinforcing the conclusion that overall damping of vibration modes involving longitudinal deformation of the fiber is significantly affected by fiber damping. Figure 6 compares the relative contributions of fiber and matrix damping, supporting the preceding observations.

### E. Prediction of Modal Damping for Thick Laminates

The dynamic macromechanical model used in the present approach uses a higher-order shear deformation laminate theory, and consequently, it is capable of better predicting the flexural vibration frequencies and modal damping capacities of thick laminates than models that do not account for this. Modal damping of a unidirectional P100/3501-6 square cantilevered laminate at room temperature was predicted for thicknesses of 2 mm ($h/a = 0.01$) and 20 mm ($h/a = 0.1$).The geometry, boundary conditions, and dynamic properties were the same in both cases. The results are summarized in Table 10. Mode shapes for modes 1–6 are the same as those in Table 6.

Comparing damping predictions for thin (Table 6) and thick (Table 10) laminates, we see that increasing the thickness of the laminate reduces the effect of fiber damping on the overall damping. Even with the treated fiber, the maximum increase in damping is 19% for the first mode, which is much smaller compared to the 250% increase for the same mode in the thin laminate.

Because of the high thickness ratio ($h/a = 0.1$), considerable shear deformation is expected in the thick laminate in all modes of vibration, reducing the fiber contribution and increasing damping caused by the matrix, because matrix shear damping is much higher than that of fiber longitudinal deformation. Note that in thick shells where fibers carry membrane loads, fiber damping could still be very important.

## IV. Conclusions

An integrated micromacromechanical model has been developed that, given the fiber and matrix dynamic properties along with the laminate geometry and boundary conditions, predicts the flexural vibration and damping parameters of the laminate. The model is based on a transversely isotropic fiber elastic property prediction model, which was extended to predict dynamic properties using the correspondence principle and the complex modulus concept. A higher-order shear deformation theory was used in conjunction with a Rayleigh–Ritz method to predict the complex modal frequencies.

Predictions of modal damping capacities for untreated and treated P100/3501-6 unidirectional eight-ply square cantilever laminate show significant contributions of the fiber to the overall damping of the laminate. Fiber contributions were found to be highest in modes exhibiting significant longitudinal deformation of the fiber, modes in which untreated fibers contributed as much as 40%, and treated fibers as much as 80%, of the total energy dissipated.

Ply orientation, temperature and thickness effects on the fiber contribution were examined. Results showed that, for similar mode shapes, ply orientation significantly altered fiber contribution to the overall damping. Fiber damping depended on temperature and, for a temperature of −50°C (corresponding to peak fiber damping), increases as high as 640% in first mode damping of unidirectional laminates were noted. Increasing thickness of the laminate reduced the effect of the fiber on overall damping of laminate flexural vibration, attributable to increased shear deformation.

## Acknowledgments

The authors gratefully acknowledge the financial assistance provided by SPARTA, Inc., Subcontract 90-189. The authors are also grateful to Dana Christiansen and Walter Whatley of SPARTA, Inc., for supplying the P100 and Hercules 3501-6 dynamic properties.

## References

[1]Jones, R. M., *Mechanics of Composite Materials*, McGraw–Hill, New York, 1975.

[2]Hashin, Z., and Rosen, B. W., "The Elastic Moduli of Fiber-Reinforced Materials," Transactions of the ASME, Series E: *Journal of Applied Mechanics*, Vol. 31, 1964, pp. 223–232.

[3]Hashin, Z., "Complex Moduli of Viscoelastic Composites—II. Fiber Reinforced Materials," *International Journal of Solids and Structures*, Vol. 6, No. 6, 1970, pp. 797–807.

[4]Gibson, R. F., "Dynamic Mechanical Properties of Advanced Composite Materials and Structures: A Review of Recent Research," *Shock and Vibration Digest*, Vol. 9, No. 2, 1989, pp. 9–17.

[5]Gibson, R. F., "Dynamic Mechanical Properties of Advanced Composite Materials and Structures: A Review," *Shock and Vibration Digest*, Vol. 19, No. 7, 1987, pp. 13–22.

[6]Chaturvedi, S. K., "Damping of Polymer Matrix Composite Materials," *Encyclopedia of Composites*, edited by S. Lee, VCH, New York, 1989.

[7]Shimansky, R., "Effect of Interfaces on Continuous Fiber Reinforced Brittle Matrix Composites," Ph.D. Dissertation, Dept. of Engineering Science and Mechanics, Pennsylvania State Univ., University Park, PA, Dec. 1989.

[8]Hashin, Z., "Analysis of Composite Materials—A Survey," Transactions of the ASME, Series E: *Journal of Applied Mechanics*, Vol. 50, Sept. 1983, pp. 481–491.

[9]Datta, S. K., Ledbetter, H. M., and Kriz, R. D., "Calculated Elastic Constants of Composites Containing Anisotropic Fibers," *International Journal of Solids and Structures*, Vol. 20, No. 5, 1984, pp. 429–438.

[10]Suarez, S. A., Gibson, R. F., Sun, C. T., and Chaturvedi, S. K., "The Influence of Fiber Length and Fiber Orientation on Damping and Stiffness of Polymer Matrix Composite Materials," *Experimental Mechanics*, Vol. 26, No. 2, 1987, pp. 175–184.

[11]Hwang, S. J., and Gibson, R. F., "Micromechanical Modeling of Damping in Discontinuous Fiber Composites Using a Strain-Energy/Finite Element Approach," *Journal of Engineering Materials and Technology*, Vol. 109, No. 1, 1987, pp. 47–52.

[12]Sun, C. T., Gibson, R. F., and Chaturvedi, S. K., "Internal Damping of Polymer Matrix Composites Under Off-Axis Loading," *Journal of Materials Science*, Vol. 20, 1985, pp. 2575–2585.

[13]Lesieutre, G. A., Eckel, A. J., and DiCarlo, J. A., "Damping of Bromine-Intercalated P-100 Graphite Fibers," *Carbon*, Vol. 29, No. 7, 1991, pp. 1025–1032.

[14]Lesieutre, G. A., Eckel, A. J., and DiCarlo, J. A., "Temperature-Dependent Damping of Some Commercial Graphite Fibers," *Metal Matrix, Carbon and Ceramic Matrix Composites 1988*, NASA CP 3018, 1988, p. 125.

[15]Lesieutre, G. A., Yarlagadda, S., Christiansen, D., and Whatley, W., "Enchanced Composite Plate Damping Using Intercalated Graphite Fiber," *AIAA Journal*, Vol. 31, No. 4, 1993, pp. 746–750.

[16]Hashin Z., "Complex Moduli of Viscoelastic Composites—I. General Theory and Application to Particulate Composites," *International Journal of Solids and Structures*, Vol. 6, No. 5, 1970, pp. 539–552.

[17]Struik, L. C. E., "Free Damped Vibrations of Linear Viscoelastic Materials," *Rheologica Acta.*, Vol. 6, No. 2, 1967, pp. 119–129.

[18]Krishnamurthy, A. V., and Vellaichamy, S., "On Higher Order Shear Deformation Theory of Laminated Composite Panels," *Composite Structures*, Vol. 8, No. 4, 1987, pp. 247–270.

[19]Whitney, J. M., *Structural Analysis of Laminated Anisotropic Plates*, Technomic, Lancaster, PA, 1987.

[20]Gorman, D. J., *Free Vibration Analysis of Beams and Shafts*, Wiley-Interscience, New York, 1975.

[21]Lin, D. X., Ni, R. G., and Adams, R. D., "Prediction and Measurement of the Vibrational Damping Parameters of Carbon and Glass Fiber-Reinforced Plastics Plates," *Journal of Composite Materials*, Vol. 18, March 1984, pp. 132–152.

E. A. Thornton
*Associate Editor*